

Introducing a New Problem: Shape-from-Silhouette when the Relative Positions of the Viewpoints is Unknown

A. Bottino, A. Laurentini, *Member, IEEE*

*Dipartimento di Automatica ed Informatica,
Politecnico di Torino,
Corso Duca degli Abruzzi, 24
10129 Torino, Italy*

andrea.bottino@polito.it, aldo.laurentini@polito.it

Tel. +39 011 5647029

Fax +39 011 5647099

Abstract

3D shapes can be reconstructed from 2D silhouettes by back-projecting them from the corresponding viewpoints and intersecting the resulting solid cones. However, in many practical cases as observing an aircraft or an asteroid, the positions of the viewpoints with respect to the object are not known. In these cases, the relative position of the solid cones is not known, and the intersection cannot be performed. The purpose of this paper is introducing and stating in a theoretical framework the problem of understanding 3D shapes from silhouettes when the relative positions of the viewpoints is unknown. The results presented provide a first insight into the problem. In particular, the case of orthographic viewing directions parallel to the same plane is thoroughly discussed, and sets of inequalities are presented which allow determining objects compatible with the silhouettes.

Keywords: Shape-from-silhouette; Volume intersection; Visual hull; Computer Vision; Object reconstruction

1 INTRODUCTION

A central problem in computer vision is understanding the shape of 3D objects from various image features. Many algorithms are based on occluding contours or silhouettes. In the latter case,

only the contours that occlude the background are considered. The rationale of this approach is that silhouettes can usually be obtained with simple and robust image processing techniques, especially with controlled background, and silhouette-based techniques do not require finding correspondences between images. It is worth noting that the problem of reconstructing an object from its silhouettes is equivalent to the problem of reconstructing the object from the shadows cast by point light sources located at the viewpoints.

Two main approaches to recovering shape from silhouettes can be identified [20]. According to one approach, the surface of the object is estimated, usually from a sequence of images obtained under known camera motion (see for instance [4], [6], [20], [21], [22]). Curved surfaces are usually considered. In several cases the motion is circular, and the object lies on a turntable ([16], [22]). Related problems are estimating camera motion ([2], [16]) and registering set of images [14]. Epipolar geometry plays a basic role in this approach.

The second approach is volumetric, and consists in building the volume \mathbf{R} shared by the regions \mathbf{C}_i (Fig. 1) obtained by back-projecting each silhouette S_i from the corresponding viewpoint. \mathbf{R} approximates the object \mathbf{O} more or less closely, depending on the viewpoints and on the shape of \mathbf{O} itself. This simple reconstruction technique, which holds for any kind of object and for any set of camera position, is called *Volume Intersection* (VI) (see [1], [4], [15], [17], [18]).

This approach requires the 3D positions of silhouettes and viewpoints. This is easy to obtain for an object on a turntable or for a mobile camera in a fixed environment, but in several practical situations this information is not available. Consider for instance objects as an aircraft, a vehicle or an asteroid. In all these cases we do not know the position and orientation of the camera in a coordinate system fixed with respect to the object. Then, the relative position of the cones produced by back-projecting each silhouettes from its viewpoint is unknown and VI cannot be performed. Even if this simple reconstruction technique is not possible, we would like to get the best of the available information.

On the ground of these considerations, this paper is aimed at introducing and exploring the problem of understanding the 3D shape of an object from a set of silhouettes (or shadows) obtained from viewpoints (or point light sources) whose relative position is not known. To the authors' knowledge this problem has not been tackled before.

The rest of this paper is organized as follows. In the next Section we review some relevant concepts. In Section 1.2 we introduce the main questions that we will investigate. In Section 2 we deal with the problem in 2D. In Section 3 we discuss the compatibility of two parallel silhouettes of 3D objects. In Section 4 we formulate a general condition for a set of silhouettes to be compatible. In Section 5 we discuss the case of three silhouettes obtained from ideal viewpoints parallel to a plane, and present sets of inequalities that must be satisfied for constructing compatible objects. In section 6 we discuss how to extend the approach to four or more silhouettes. Techniques for computing feasible VI parameters are outlined in Section 7, together with the simplification introduced by polygonal silhouettes. Section 8 contains open problems and concluding remarks.

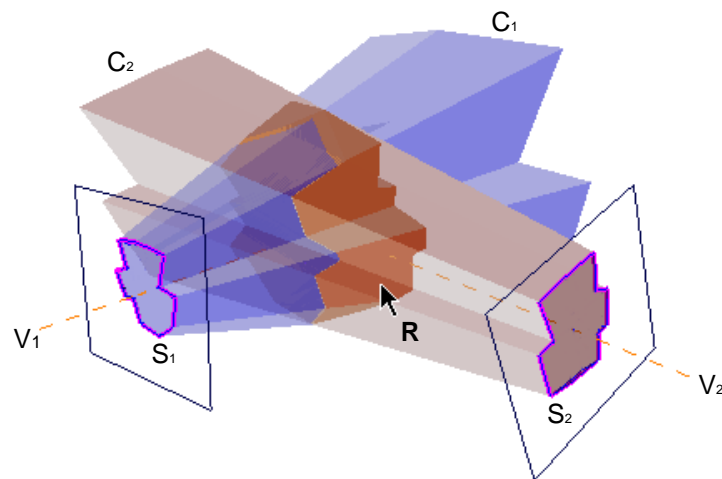


Fig. 1 – The volume intersection technique

1.1 Visual hull and hard points

In this section we briefly review some definitions relevant to our problem. First, the concept of *visual hull* of an object [8], [9], [10] allows answering questions such as: can the shape of an object be fully understood from its silhouettes? If not, which is the closest approximation that can be obtained? Can an object be distinguished from another using silhouettes only? The visual hull is the object that can be obtained by VI using all the viewpoints that belong to a viewing region completely enclosing the original object without entering its convex hull. It is also the largest object that produces the same silhouettes as the given object.

The answers to the previous questions are as follows. An object can be reconstructed from its silhouettes iff it is coincident with its visual hull. The closest approximation that can be obtained is the visual hull. We can tell an object from another using silhouettes iff their visual hulls are different.

Another tool for the shape-from-silhouette approach is the concept of *hard point* [9]. A point of the surface of the reconstructed object \mathbf{R} from a set of silhouettes and viewpoints is hard if it belongs to any object that produces the same silhouettes from the same viewpoints. The concept of hard point allows stating a necessary condition for the reconstruction to be optimal, i.e. the visual hull, and is at the basis of interactive VI algorithms [3].

1.2 The main questions

In the following, for brevity, we will use the expression “set of silhouettes” to specify a set of silhouettes together with the position of the corresponding viewpoint with respect to each silhouette. These data, corresponding to the pinhole camera model, allow constructing a solid cone for each silhouette, but not positioning the cones in the 3D space.

For understanding how the 3D shape is related to such a set of silhouettes, two main questions can be considered.

The first question is: given a set of silhouettes, does an object exist able to produce them? For instance, does an object exist able to produce the three orthographic silhouettes (or shadows) of Fig. 2?

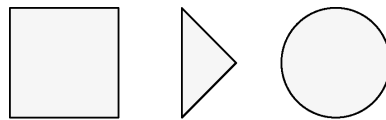


Fig. 2 - Are these orthographic silhouettes compatible? (See Section 4 for the answer)

We will call *compatible* a set of silhouettes if the same object can generate them. An object able to produce a compatible set of silhouettes will be said to be compatible with the set.

The second question is the main practical issue: how can we find one or more compatible objects given a compatible set of silhouettes, as that produced by a real object.

Let us recall that shape-from-silhouettes at most allows constructing the visual hull of an object. Infinite objects can have the same visual hull. In the following, when not otherwise explicitly stated, we will use the expressions ‘object’ and ‘compatible object’ referring to an object reconstructed by VI. The reconstructed object could be the visual hull of the real object, and in any case satisfies the properties of a visual hull (see [8]). For instance, in 2D by VI we can only construct convex objects. Equivalently, in 2D all visual hulls are convex, or consist of convex parts if not connected.

Although we have not been able to find completely general answers to the previous questions, we will present a set of results that provide a first insight into the problem.

2 THE PROBLEM IN 2D

The problem of reconstructing 2D objects from one-dimensional parallel or perspective silhouettes with completely known viewpoints has been analysed in the research area known as

geometric probing. Optimal interactive strategies for reconstructing convex polygons (or, using the concept of visual hull, the visual hull of general polygons) have been presented in [11] and [12]. For a survey of geometric probing problems and results, the reader is referred to [19].

Let us consider now the case of unknown relative position of the viewpoints for both perspective and parallel projections in 2D. In the following we will restrict ourselves to consider only connected objects.

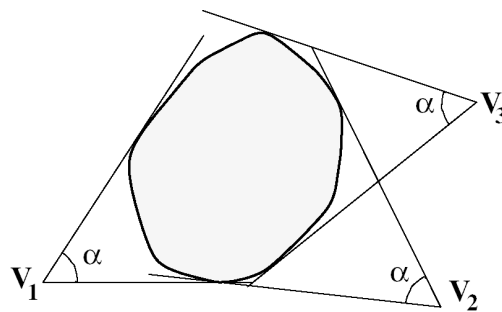


Fig. 3 - 2D perspective projections

Perspective projection. A perspective projection of a 2D object is essentially an angle. If we neglect the facts that a real object cannot lie too close to a real camera, and the image size is limited, any convex object can produce any angle between 0 and π (Fig. 3). Vice-versa, a set of such angles does not provide any information about the originating objects. It is easy to answer the questions raised in the introduction. It is clear that any set of silhouettes is compatible. We can very easily construct compatible objects: any object will do. In other words, such silhouettes provide no information at all.

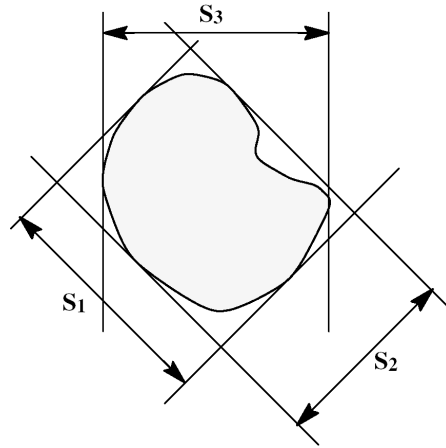


Fig. 4 - 2D parallel projections

Parallel projections. In this case, the silhouettes are line segments (Fig. 4), which can be sorted by length from S_{\min} to S_{\max} . It is easy to see that:

Proposition 1. *If a connected object produces two parallel silhouettes of lengths S' and S'' ($S' < S''$), it can also produce any silhouette of length S such that $S' < S < S''$*

We omit a formal proof of this obvious statement. It follows that only S_{\min} and S_{\max} are significant. It is easy to construct compatible objects. First, let us choose at random the angle α between the viewing directions (Fig. 5a). The parallelogram obtained by intersection is a possible compatible object. Infinitely many other compatible objects, enclosed by the parallelogram, exist. Examples are shown in Fig. 5b.

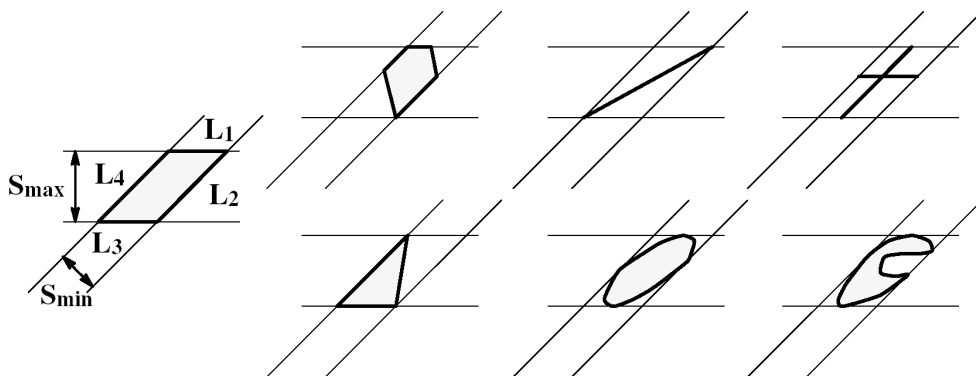


Fig. 5 - Objects compatible with S_{\min} and S_{\max}

The two rightmost objects of the figure are not visual hulls (as already noted, all connected 2D visual hulls are convex), and cannot be generated by volume intersection. It is clear that all the compatible objects must share at least one point with each edge of the parallelogram. If we consider, as we currently do in this paper, only visual hulls, a compatible object is any convex object enclosed by the parallelogram and sharing at least one point with each edge. Any such object is able to produce, with suitable viewing directions, any silhouettes between S_{\min} and S_{\max} . Clearly, this simple construction is possible for any pair (S_{\min}, S_{\max}) . It follows that any set of silhouettes is compatible.

We can conclude that, without any other shape clue, 2D silhouettes supply very little shape information without the relative position of the viewpoints!

3 COMPATIBILITY OF TWO ORTHOGRAPHIC SILHOUETTES OF 3D OBJECTS

In the rest of this paper we will restrict ourselves to consider simply connected 3D objects and their orthographic projections. This approximates the practical case of objects small with respect to their distance from the camera.

First, we will investigate the compatibility of two silhouettes. Let S be a 2D orthographic silhouette of a 3D object. Let us project orthographically S along a direction in the plane of S . The 1D silhouette obtained depends on the angle α that the chosen direction makes with the x axis of a coordinate system fixed with respect to S (Fig. 6).

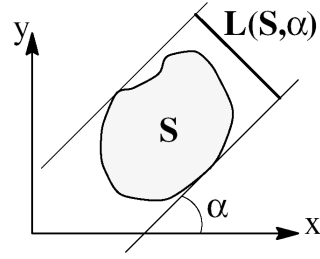


Fig. 6 - The 1D silhouette $L(S, \alpha)$ of a 2D silhouette

Let $L(S, \alpha)$ be the length of the 1D silhouette of S . By rotating the projection direction from 0 to π we obtain all possible values of $L(S, \alpha)$. The following statement holds.

Proposition 2. A necessary and sufficient condition for two orthographic silhouettes S_1 and S_2 to be compatible is that two angles α_1 and α_2 exist such that $L(S_1, \alpha_1) = L(S_2, \alpha_2)$.

Proof. Let us consider the parameters required for intersecting in 3D the cylinders obtained by back-projecting S_1 and S_2 . First, we must select the angle β between the viewing directions, or, which is the same, the angle between the planes of the silhouettes. Next, we must locate both silhouettes in these planes. Let L be the intersection of the planes. For positioning S_1 it is sufficient to select the angle between its coordinate system and L . Positioning S_2 requires to choose: i) the angle of its coordinate system with respect to L ; ii) the distance with respect to S_1 measured along L . Translating S_2 along the direction orthogonal to L does not affect the intersection result.

Now let us show that the condition is sufficient. Fig. 7(a) shows how to perform the VI for each pair (α_1, α_2) that satisfies this condition. The two cylinders must be positioned as follows:

- The 2D viewing directions that produce $L(S_1, \alpha_1)$ and $L(S_2, \alpha_2)$ must be both orthogonal to L
- Both cylinders must be supported by the same plane P orthogonal to L

It is clear from the figure that the object obtained by VI is compatible with both silhouettes. This reconstruction is possible for any angle β between the viewing directions.

Let us show that the condition is necessary. Let again $L(S_1, \alpha_1)$ and $L(S_2, \alpha_2)$ be the 1D silhouettes obtained with viewing directions normal to L . They are different for any possible choice of α_1 and

α_2 . Without loss of generality, assume $L(S_1, \alpha_1) > L(S_2, \alpha_2)$. Fig. 7(b) shows that, whatever the distance along L between S_1 and S_2 , the object obtained by VI cannot be compatible with S_1 . At most, it is compatible with S_2 , as in the case shown in the figure. Since this happens for any choice of the intersection parameters, the condition is also necessary.

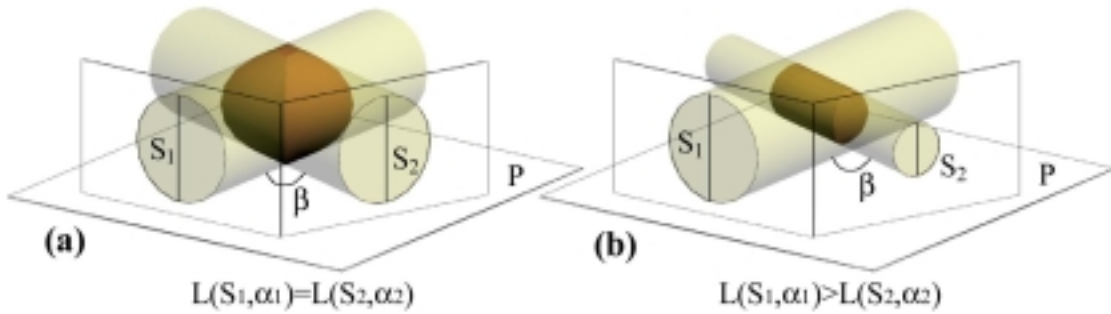


Fig. 7 - In (a) it is shown how to find an object compatible with two silhouettes having two equal 1D projections. If this condition is not satisfied, the silhouettes are not compatible (b).

Observe that the necessary part of the statement could be also obtained considering epipolar tangency.

In general, the reconstruction can be performed for an infinite number of pairs (α_1, α_2) . This means that, if the condition is verified, ∞^2 compatible objects can be constructed. The number of objects reduces to ∞^1 if the 1D projections are equal for only one pair (α_1, α_2) .

4 COMPATIBILITY OF 3 OR MORE ORTHOGRAPHIC SILHOUETTES

We have shown that verifying if two orthographic silhouettes are compatible, and constructing compatible objects, is easy. But how can we find if three or more silhouettes are compatible? Clearly, we have that:

Proposition 3. A necessary condition for a set of silhouettes to be compatible is that all pairs of silhouettes of the set are compatible.

Is this condition also sufficient? In the example of Fig. 8, three silhouettes satisfying this condition can be combined -in one way only- to produce a compatible object, a cylinder cut by two skew planes (the plane P is normal to both S_1 and S_2). However, another example will show that in general the condition is not sufficient.

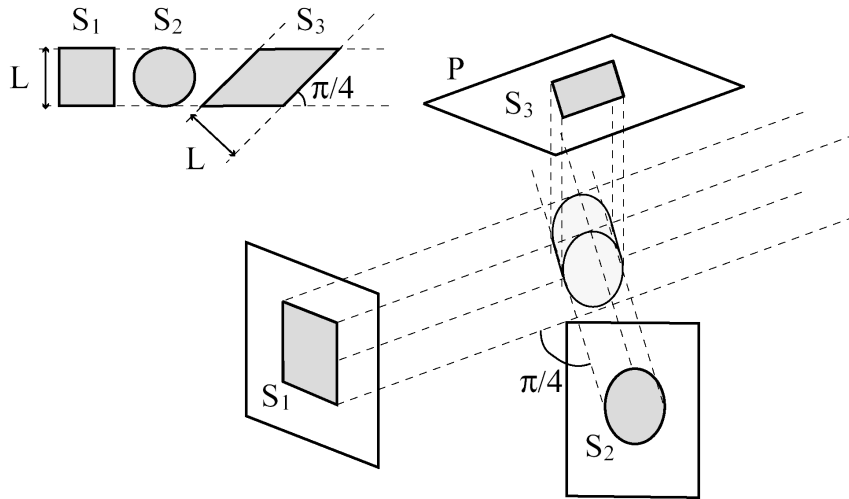


Fig. 8 - In this case, S_1 , S_2 and S_3 determine only one compatible object.

Let us go back to the three orthographic silhouettes of Fig. 2. The exact sizes of S_1 , S_2 , S_3 are shown in Fig. 9.

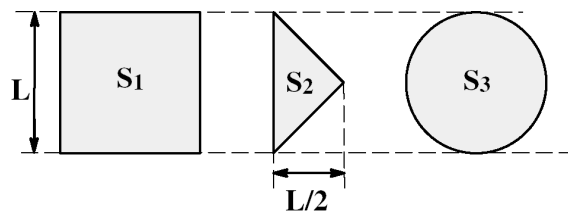


Fig. 9 - Three silhouettes that are pairwise compatible

The silhouettes are pairwise compatible. In addition, the L functions of their 1D projections have only one value in common, that is L , they only share one value, that is L , of their 1D projections, since:

$$L \leq L(S_1, \alpha_1) \leq L\sqrt{2}$$

$$L/2 \leq L(S_2, \alpha_2) \leq L$$

$$L(S_3, \alpha_3) = L$$

Let us intersect first the cylinders produced by back-projecting the square S_1 and the triangle S_2 (Fig. 10) according to the rules of Fig. 7(a). In this case, we can choose at random the angle β only.

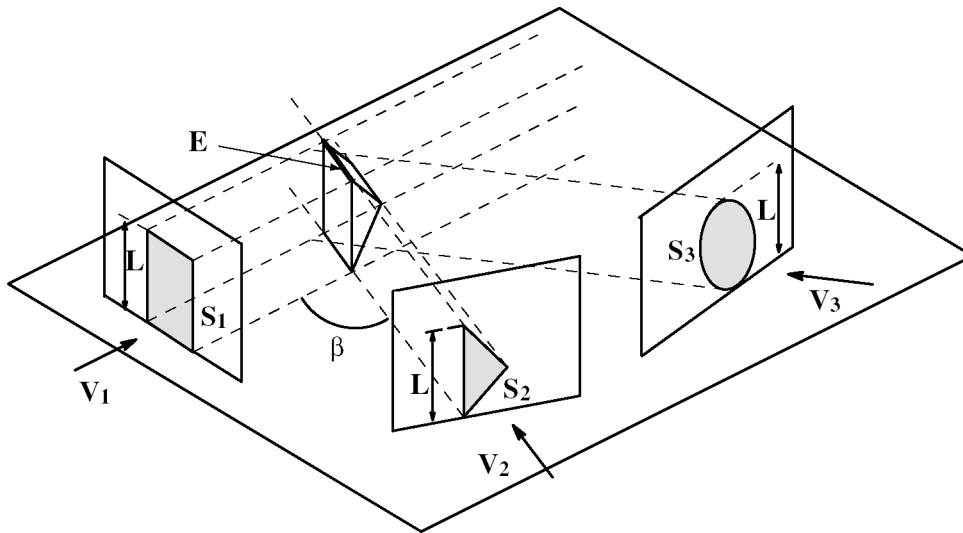


Fig. 10 - The silhouettes of Fig. 9 are not compatible

Let us consider the third cylinder produced by the circular silhouette. To satisfy the conditions of Fig. 7(a) with respect to both S_1 and S_2 , the same plane must support the three cylinders (see Fig. 10). Let E be the upper edge of the polyhedron resulting from the first intersection. The intersection with the third cylinder should cut away some parts of this polyhedron, but the edge E must not be affected, otherwise a silhouette smaller than S_1 would be obtained from V_1 . We can say that, for each β , the corresponding E is hard. But the only way for this edge to be not affected by the second intersection is to choose $V_3=V_2$, and to locate the third cylinder so as to superimpose the lines which project the top points of S_2 and S_3 . This preserves the edge E , but produces a contradiction, since obviously an object cannot produce two different silhouettes with the same viewpoint. Then, in general, to be compatible in pairs is not sufficient for a set of silhouettes to be compatible.

For a closer insight into the problem of silhouette compatibility, it will be helpful to consider one property of the object \mathbf{R} reconstructed by VI. Let us consider one of the silhouettes involved in the process, the corresponding viewing direction V and the cylinder circumscribed to the object \mathbf{O} made of lines parallel to this direction (Fig. 11).

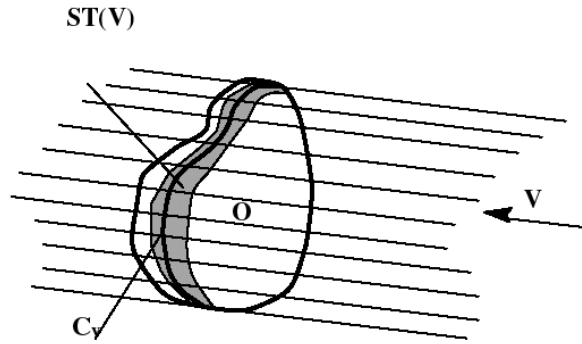


Fig. 11 - The strip $ST(V)$ and the curve C_v

Each line of this cylindrical surface must share with the surface of \mathbf{O} at least one point. These points form a curve C_v . This curve belongs to an annular surface homeomorphic to a closed curve, a strip $ST(V)$ of variable width (measured along a line of the cylinder), which is what is left of the original circumscribed cylinder after the various intersections. During the reconstruction process, this annular strip cannot be interrupted (i.e. become homeomorphic to an open curve); at most it can reduce to a curve with zero width. In this case, the curve consists of hard points. In fact, this is the general condition we have implicitly applied discussing the example of Fig. 10, since the edge E belongs to the strip $ST(V_1)$.

Then we can formulate the following condition for the VI algorithm to be feasible:

Proposition 4. A necessary and sufficient condition for a set of silhouettes to be compatible is that it be possible to find viewpoints such that no annular strip of the reconstructed object is interrupted.

In the next sections this condition will be used for constructing algorithms both for verifying the compatibility of a set of silhouettes and reconstructing compatible 3D objects.

5 THREE SILHOUETTES WITH VIEWING DIRECTIONS PARALLEL TO A PLANE: COMPATIBILITY AND RECONSTRUCTION

In this section we deal with a particular case of the general problem, where all viewing directions are parallel to the same plane (Fig. 12). This case idealizes some practical situations, as observing a vehicle on a planar surface, or a ship on a calm sea. Clearly, all silhouettes have the same height and the same plane must support all cylinders obtained by back-projection. We will show that applying the condition of Proposition 4 allows writing sets of inequalities that determine feasible VI parameters. We will also see that the number of sets of inequalities, as well as the number of inequalities in each set, quickly increases with the number of silhouettes.

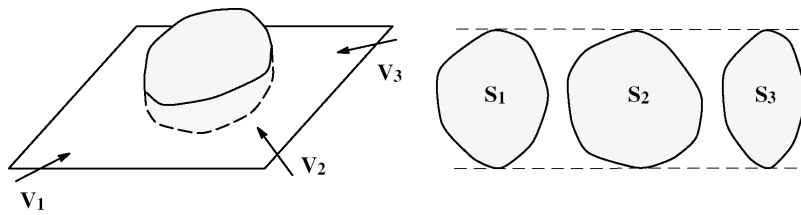


Fig. 12 - Viewing directions parallel to the same plane

We consider first the compatibility of three silhouettes S_1 , S_2 and S_3 . Let us introduce some notation (see Fig. 13). Each planar silhouette S_i is defined, for $0 \leq y \leq y_{\max}$ by two curves $S_{il}(y)$ and $S_{ir}(y)$. For simplicity, let us consider mono-valued functions. Also let $S_i(y) = S_{ir}(y) - S_{il}(y)$.

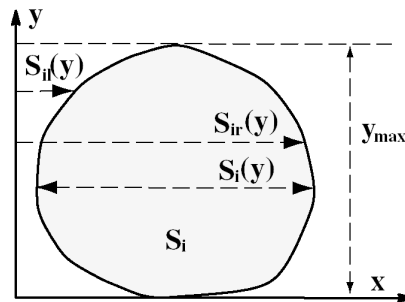


Fig. 13 - Notations used for a silhouette.

Three cases, related to the shape of the silhouettes, will be considered. The first case is more general and requires three intersection parameters. The second and third are sub-cases of the first, involving two and one parameter respectively. For all of them the condition of Proposition 4 will produce various sets of inequalities involving the intersection parameters.

5.1 Silhouettes with flat top and bottom

This case, depicted in Fig. 14, refers to silhouettes such that

$$S_{ir}(0) \neq S_{il}(0) \text{ and } S_{ir}(y_{\max}) \neq S_{il}(y_{\max}) \quad \forall i.$$

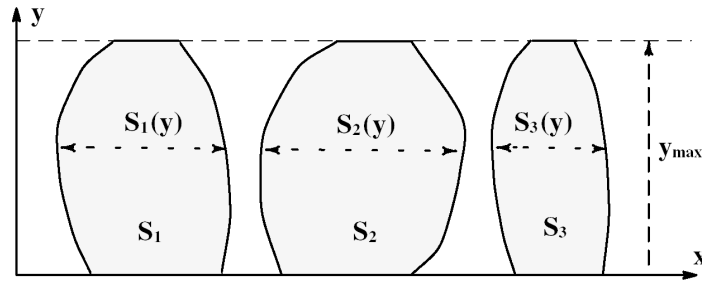


Fig. 14 - Silhouettes with flat top and bottom

Let us consider a horizontal plane corresponding to a value of y between 0 and y_{\max} , and its intersection with the three cylinders obtained by back-projecting the silhouettes. Let us consider in this plane the arrangement of the 2D silhouettes $S_1(y)$, $S_2(y)$, $S_3(y)$ and of the viewpoints V_1, V_2, V_3 shown in Fig. 15(a). Other arrangements of viewpoints and silhouettes that could satisfy the condition of Prop.4 are possible, and will be discussed at the end of this Section.

It is not difficult to see that, in the case in Fig. 15, Prop. 4 requires that the two lines projecting the endpoints of $S_3(y)$ along the direction V_3 must lie inside the two areas highlighted in Fig. 15(a). For the whole silhouettes to be compatible, this must hold for all y .

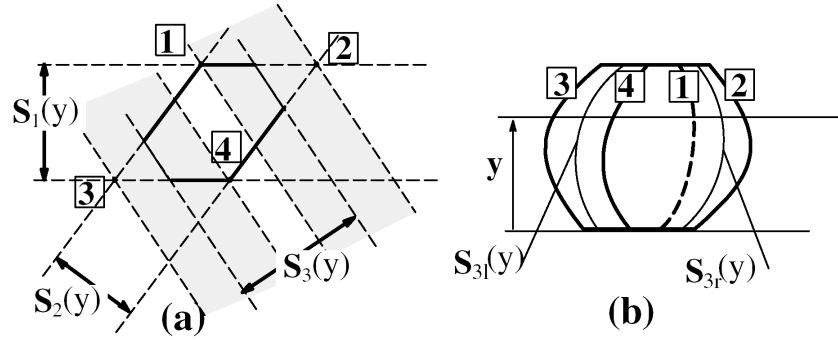


Fig. 15 - (a) A case where $S_3(y)$ is compatible with $S_1(y)$ and $S_2(y)$ in a horizontal plane. (b) The condition for the compatibility of the whole silhouettes.

This means that, if we project orthographically onto the plane of S_3 for all y the vertices of the parallelogram marked **1, 2, 3** and **4** in Fig. 15(a), we should obtain a layout as that shown in Fig. 15(b). For the reconstruction to be possible, $S_{3l}(y)$ must lie between the two leftmost curves, in this case the projections of the vertices **3** and **4**, and $S_{3r}(y)$ must lie between the two rightmost curves, the projections of the vertices **1** and **2**.

To derive the set of inequalities that define for this case feasible intersection parameters, let us inspect in more detail the intersection in a horizontal plane (Fig. 16). Let O_1, O_2, O_3 be the intersections of the axes y of the coordinate system of each silhouette with this plane. Intersecting $S_1(y)$ and $S_2(y)$ requires to fix an angle, let it be α_1 . Intersecting also $S_3(y)$ requires choosing two more parameters: the angle α_2 and a distance, let it be d (see Fig. 17). d is the distance between two points lying on the line projecting O_1 along the direction V_1 . The first point is the intersection of this line with the line projecting O_2 along V_2 , and the second is the intersection with the line projecting O_3 along V_3 . Thus, to find feasible solutions we must search the 3-dimensional space $[\alpha_1, \alpha_2, d]$.

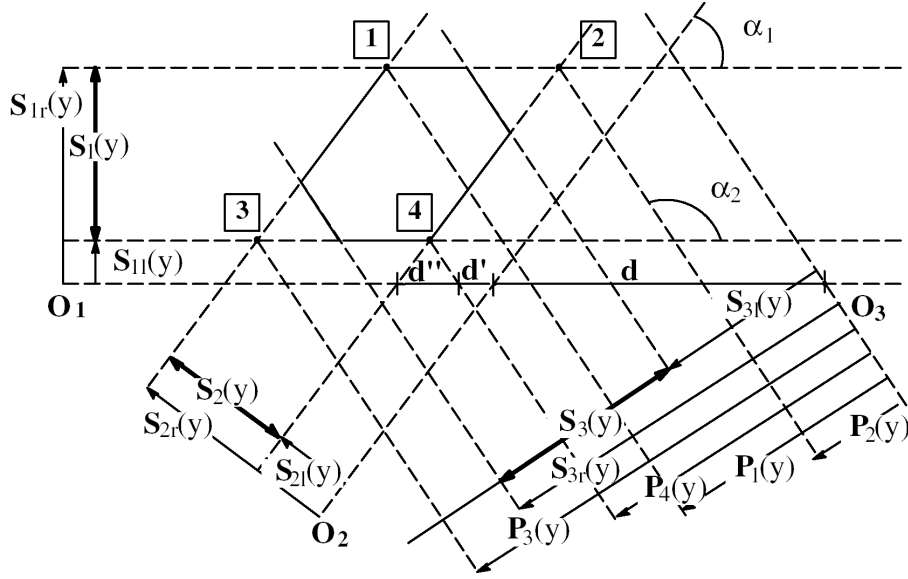


Fig. 16 - The intersections in a horizontal plane

Let $P_1(y)$, $P_2(y)$, $P_3(y)$ and $P_4(y)$ be the distances from O_3 of the orthographic projections of the vertices of the parallelogram onto the line supporting $S_3(y)$. The compatibility condition for the three silhouettes is expressed by the following inequalities, which can be worked out from the figure.

$$\begin{aligned}
 S_{3r}(y) &\geq P_4(y) = (d + d') \cos(\alpha_2 - \pi/2) \\
 S_{3r}(y) &\leq P_3(y) = P_4(y) + (S_2(y) / \cos(\alpha_1 - \pi/2)) \cos(\alpha_2 - \pi/2) \\
 S_{3l}(y) &\geq P_2(y) = P_4(y) - (S_1(y) / \cos(\alpha_2 - \pi/2)) \cos(\alpha_2 - \alpha_1 - \pi/2) \\
 S_{3l}(y) &\leq P_1(y) = P_2(y) + (S_2(y) / \cos(\alpha_1 - \pi/2)) \cos(\alpha_2 - \pi/2) \\
 P_4(y) &\geq P_1(y)
 \end{aligned} \tag{1}$$

where

$$\begin{aligned}
 d' &= S_{2l}(y) \cos(\pi/2 - \alpha_1) - d'' \\
 d'' &= S_{1l} \sqrt{1/\cos^2(\pi/2 - \alpha_1) + 1/\cos^2(\pi/2 - \alpha_2) + 2 \frac{\cos^2(\alpha_2 - \alpha_1)}{\cos(\pi/2 - \alpha_1) \cos(\pi/2 - \alpha_2)}}
 \end{aligned}$$

In (1), the purpose of the fifth inequality is to characterize the case just analysed, let it be Case 1. Seven other cases are possible, each producing different sets of inequalities. The cases are determined by the direction of V_3 with respect to V_1 , V_2 , and the directions of the diagonals V_{14} and V_{32} of the parallelogram, as shown in Fig. 17.

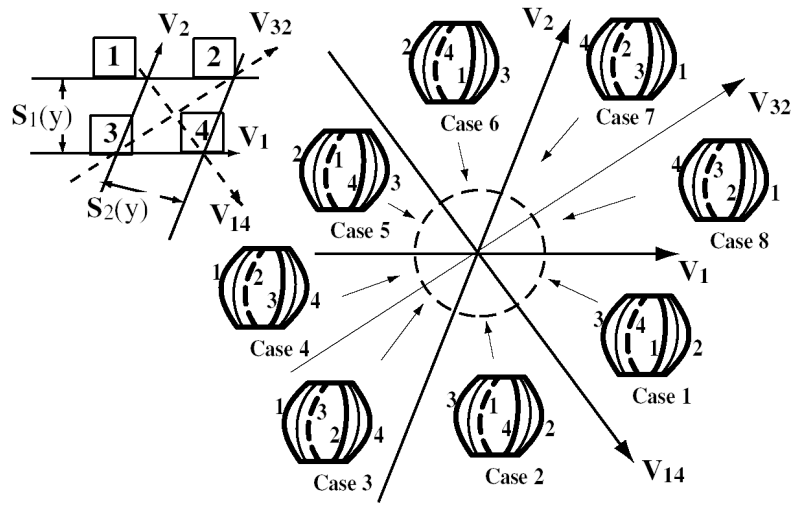


Fig. 17 - The eight intersection cases

Case 1 refers to an ideal viewpoint V_3 that, for each y , is enclosed between the directions opposite to V_{14} and V_1 . In Case 2, V_3 lies between V_2 and the direction opposite to V_{14} ; in Case 3, between V_{32} and V_2 , and so on. For each case, a possible orthographic projection onto the plane of S_3 of the edges of the object produced by the first intersection is shown with thick lines. The boundaries of S_3 are the thin lines. Observe that cases where the directions of V_3 are opposite, as Case 1 and Case 5, in general produce different sets of inequalities. The inequalities turn out to be equal only if S_1 , S_2 and S_3 are symmetric with respect to a vertical central axis.

The inequalities corresponding to the various cases are easily written. For instance:

Case 2

$$\begin{aligned}
 S_{3r}(y) \leq P_3(y) \quad S_{3r}(y) \geq P_1(y) \quad S_{3l}(y) \leq P_4(y) \quad S_{3l}(y) \geq P_2(y) \\
 P_1(y) \geq P_4(y)
 \end{aligned} \tag{2}$$

The expressions of $P_i(y)$, $i=1, \dots, 4$, are as those in inequalities (1). We omit for brevity the inequalities corresponding to the other cases.

It is important to observe that, in general, the directions of the diagonals V_{14} and V_{32} depend on y . This means that, for a given vector of intersection parameters, two of the previous cases could take place for different values of y for the same object. An example is shown in Fig. 18. For $y < y^*$ we have Case 2, for $y > y^*$ Case 1.

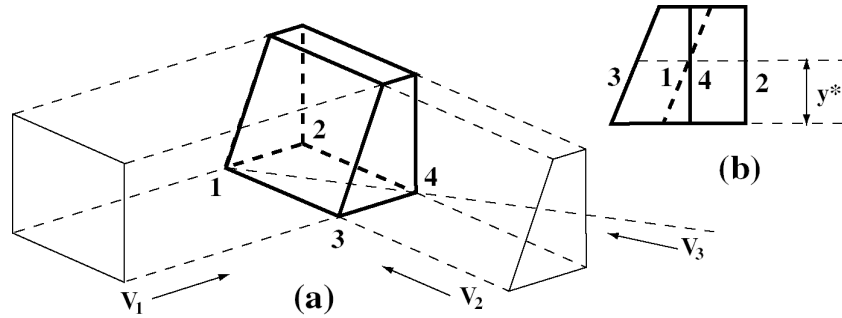


Fig. 18 - An example where, for the same V_3 and different y , two different cases take place (a). The orthographic projection onto the plane of S_3 is shown in (b)

Then, the eight cases can be grouped into four sets of two cases each. The sets are: (1,2), (3,4), (5,6), (7,8). The two cases of each set can take place for the same object. For each y , the parameters of a feasible intersection should satisfy the inequalities corresponding to either case of one set.

5.2 Silhouettes with one flat end

In this sub-case we have (Fig. 19):

$$S_{ir}(0) \neq S_{il}(0) \text{ and } S_{ir}(y_{\max}) = S_{il}(y_{\max}) \quad \forall i.$$

This is, for instance, the case of a ship, whose silhouettes has a flat bottom and one upper point, the top of the mast. We have that:

-The intersection only depends on two parameters, α_1 and α_2 , since d is uniquely determined by these angles. In particular, if the vertical axis y passes through the upper points of each silhouette as in Fig. 19, we obtain $d=0$ (see Fig. 16).

-The 8 sets of inequalities of the previous subsection (with $d=0$) hold, and they can be grouped into four sets of two cases each as before.

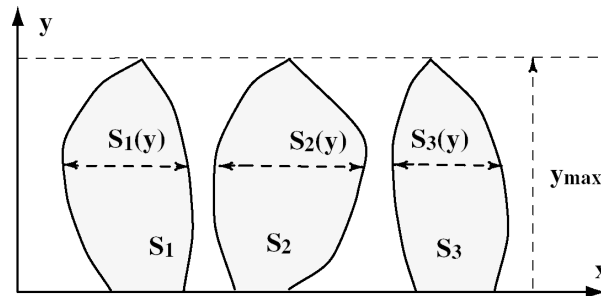


Fig. 19 - Silhouettes with flat bottom

5.3 Silhouettes without flat ends

Let us assume:

$$S_{ir}(0) = S_{il}(0) \text{ and } S_{ir}(y_{\max}) = S_{il}(y_{\max}) \quad \forall i.$$

This is a sub-case of the case of the previous section. Let us again assume that, for each silhouette, the origin of the axes is coincident with the upper point. Also let l_i , $i=1,2,3$, be the abscissas of the lower points (Fig. 20).

It is easily seen that the intersection only depends on α_1 , which determines two possible pairs of values of α_2 .

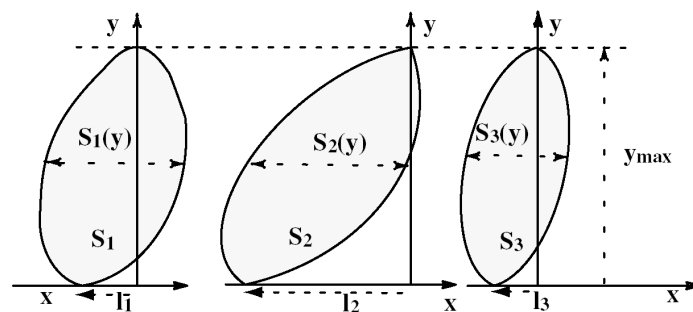


Fig. 20 - Silhouettes without flat ends

In fact, let us consider the plane $y=0$, containing the three lower points of the silhouettes (Fig. 21). The two possible viewing directions V'_3 and V''_3 are those which project exactly onto l_3 the segment l in the figure. V'_3 and V''_3 form the angles α'_2 and α''_2 with V_1 .

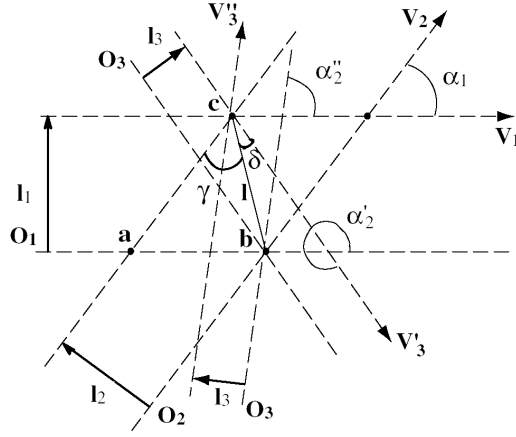


Fig. 21 - The plane $y = 0$

From the triangle whose vertices are marked a , b and c in the figure we obtain:

$$l = \sqrt{(1/\sin^2 \alpha_1)(l_1^2 + l_2^2 - 2l_1 l_2 \cos \alpha_1)}$$

$$\gamma = \arccos((\sin \alpha_1 / 2ll_1)(l^2 + (l_1^2 / \sin^2 \alpha_1) - (l_2^2 / \sin^2 \alpha_1)))$$

We also have:

$$l_3 = l \sin \delta$$

It follows that the two possible values of α_2 are:

$$\alpha'_2 = \gamma + \alpha_1 + \arcsin(l_3/l) + \pi \quad (3)$$

$$\alpha''_2 = \gamma + \alpha_1 - \arcsin(l_3/l) \quad (4)$$

Concluding, 16 sets of inequalities depending on one parameter only result. They are obtained by substituting the two previous expressions of α_2 in each set of inequalities of sub-section 5.1.

6 THE INEQUALITIES FOR MORE THAN THREE SILHOUETTES

This section deals with the set of inequalities that define feasible intersection parameters for more than 3 orthographic silhouettes with viewpoints parallel to the same plane.

6.1 Silhouettes with flat top and bottom

Let us consider any of the eight cases described in subsection 5.1, for instance Case 1, and let us add a fourth silhouette S_4 . In each horizontal plane $S_1(y)$, $S_2(y)$ and $S_3(y)$ produce a polygon with six vertices and three pairs of parallel edges (see Fig. 22). The new intersection is defined by two more parameters, the angle α_3 between V_1 and V_4 and the distance d_l , measured, as d , along the line that projects O_1 from V_1 . Satisfying the condition of Proposition 4 requires, in each horizontal plane, to cut away two opposite vertices, without eliminating completely the edges that meet at these vertices. For instance, let us select the opposite vertices **7** and **5**. In this case, we cannot cut away completely the edges **17**, **78**, **65** and **54**.

By orthographically projecting the six vertices onto the plane of S_4 we obtain six curves. For the new intersection to be feasible, the boundaries $S_{4l}(y)$ and $S_{4r}(y)$ of S_4 must lie in the areas bounded by the two leftmost and the two rightmost curves respectively.

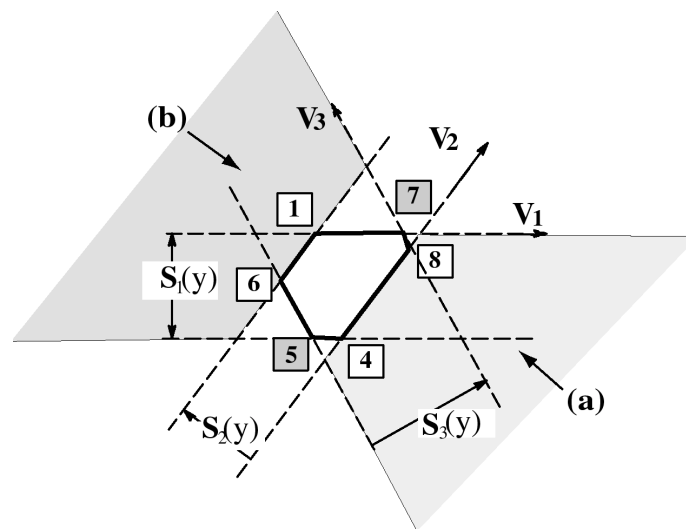


Fig. 22

Various sets of inequalities result, depending on the direction of V_4 with respect to V_1, V_2, V_3, V_{18} , and V_{64} . First, let us distinguish two cases (case **(a)** and **(b)** of Fig. 22) related to the directions (V_{56}, V_{54}) and (V_{17}, V_{78}) which determines the leftmost and rightmost vertices (respectively, **5** and **7** for case **(a)** and **7** and **5** for case **(b)**). In each case we have four sub-cases for the leftmost and rightmost strips where S_{4l} and S_{4r} must lie (see Fig. 23). The inequalities corresponding to each sub-case are easily written. For instance, for the sub-case **a₁** it is:

$$P_5(y) \leq S_{3l}(y) \quad S_{3l}(y) \leq P_4(y)$$

$$P_1(y) \leq S_{3r}(y) \quad S_{3r}(y) \leq P_7(y)$$

$$P_4(y) \leq P_6(y) \quad P_8(y) \leq P_1(y)$$

where $P_i(y)$ are the projections of the points $i(y)$ onto the plane of S_4 . The first four inequalities states that the boundaries of S_4 lies into the areas bounded by the two rightmost ($P_5(y)$ and $P_4(y)$) and leftmost ($P_1(y)$ and $P_7(y)$) curves. The last two inequalities guarantee that the inner boundaries of these areas are actually $P_6(y)$ and $P_8(y)$.

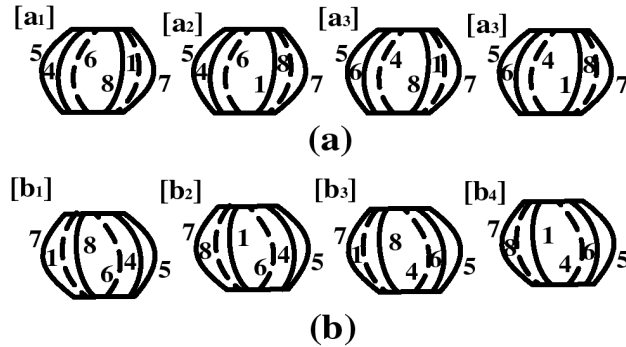


Fig. 23 - Cases (a) and (b) and the 8 sub-cases

For brevity, we will not report here the expressions of $P_i(y)$ as functions of the five parameters $\alpha_1, \alpha_2, \alpha_3, d$ and d_1 .

Let us observe that the directions of the diagonals, which determine the various sub-cases, are in general different for different values of y . This means that the sub-cases can be grouped into two

sets, $(\mathbf{a}_1, \mathbf{a}_2, \mathbf{a}_3, \mathbf{a}_4)$ and $(\mathbf{b}_1, \mathbf{b}_2, \mathbf{b}_3, \mathbf{b}_4)$. Each of the cases in either set can take place for the same object at different y .

Summarizing, each set of inequalities that defines feasible intersection parameters for four silhouettes contains 11 inequalities:

1. the five inequalities of Section 4
2. six new inequalities also referring to S_4

As for the number of sets of inequalities, we have 8 cases for three silhouettes, 3 pairs of opposite vertices and 8 cases for each pair, and thus 192 sets each containing 11 inequalities.

Five or more silhouettes

The previous discussion about the fourth silhouette does hold for any further silhouette. In fact, we must always cut a pair of opposite vertices without deleting completely the edges converging at these edges. It follows that

- each new silhouette adds two parameters, seven inequalities for each case. Thus, for n silhouettes, the number of parameters is $2n-3$, and the number of inequalities $6(n-3)+5$ ($n \geq 3$).
- each silhouette adds 8 sub-cases for each pair of opposite vertices. For the n -th silhouette, the pair of vertices are $n-1$. Let $N_c(n)$ be the number of sets of inequalities for n silhouettes. For $n > 3$ it is: $N_c(n) = 8(n-1)N_c(n-1)$. Therefore we must face an exponential growth of the number of cases.

6.2 Silhouettes with one flat end

The sets of inequalities are similar to those described in the previous sub-section. The only difference is that each new silhouette introduces only one new parameter, an angle, since all

distances d_i are zero if for each silhouette the axis y passes through the upper point. Therefore, for n silhouettes the parameters are $n-1$.

6.3 Silhouettes without flat ends

In this case, the inequalities depend on one parameter only, the angle α_1 . Let $N'_c(n)$ be the number of sets of inequalities. For each new silhouette S_n two intersection parameters are possible, determined by equations (3) and (4) with l_n substituting l_3 . It follows that $N'_c(n) = N_c(n) 2^{(n-2)}$

7 SOLVING THE INEQUALITIES

The inequalities discussed in the previous section allow to answer, in a particular case, both question raised in the introduction: finding objects compatible with a set of compatible silhouettes, and understanding if an (artificial) set of silhouettes is compatible.

Developing computer algorithms able to deal with these non-linear inequalities is outside the scope of this work, and will be the object of future development. However, we will briefly discuss how this problem can be addressed.

A technique for finding the feasible solution set \mathbf{S} of a set of non-linear inequalities is presented in [13]. This technique, which also takes into account data uncertainty, is based on paving the parameter space with boxes whose dimensions are related to data uncertainty, and has been implemented and tested.

This technique can be used for finding feasible parameter sets for one value of y between 0 and y_{\max} . Each feasible parameter set corresponds to a group of inequalities that can take place for the same object. If one of the parameter set is empty, the corresponding group of inequalities can be discarded. Otherwise, we could perform an incremental computation, adding each time (or

subtracting) a small Δy , related to data uncertainty and to the shape of the silhouettes, to the previous y . For each group of inequalities, the new feasible parameter set at $y+\Delta y$ must be a subset of the feasibility set at y . So, each time the computation should be reduced.

7.1 Polygonal silhouettes

Reconstruction with polygonal silhouettes results in a substantial simplification of the computation. In this case, using horizontal lines passing through all vertices of the silhouettes, we obtain a set of horizontal strips such that in each strip each slice of silhouette is bounded laterally by two segments (see Fig. 24).

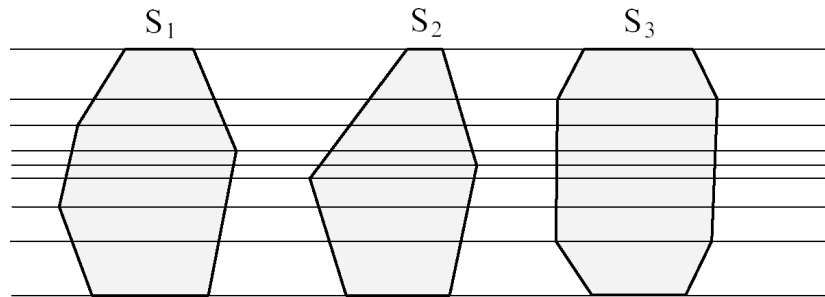


Fig. 24 – Dividing polygonal silhouettes into strips

Consider the inequalities for N silhouettes and a given vector \mathbf{I}^* of intersection parameters. It is easy to see that both sides of each inequality depends linearly on the silhouettes boundaries S_{il} and S_{ir} , $i=1, \dots, N$. As a matter of facts, both the coordinates of the $2N-2$ vertices of the polygon due to the first $N-1$ silhouettes and their projection P_j along a fixed direction onto a line normal to V_n depend linearly on S_{il} and S_{ir} , $i=1 \dots N-1$. It follows that, if the inequalities hold at both the minimal and maximal y values of a strip for the same intersection parameters \mathbf{I}^* , they also hold for \mathbf{I}^* for any value of y within the strip. This statement holds even if \mathbf{I}^* belongs to the feasibility sets of two different sets of inequalities. This can be easily seen considering the example in Fig. 25. The figure on the left refers to case \mathbf{a}_1 of Fig. 23 at both ends of the strip. In the figure on the right we have case \mathbf{a}_1 at the top and \mathbf{a}_3 at the bottom. It is clear that, if S_{il} and S_{ir} satisfy the inequalities (in other

words they lie in the rightmost and leftmost intervals between the points projections of the vertices) at the top and the bottom of the strip, they also satisfy the inequalities for any y in between.

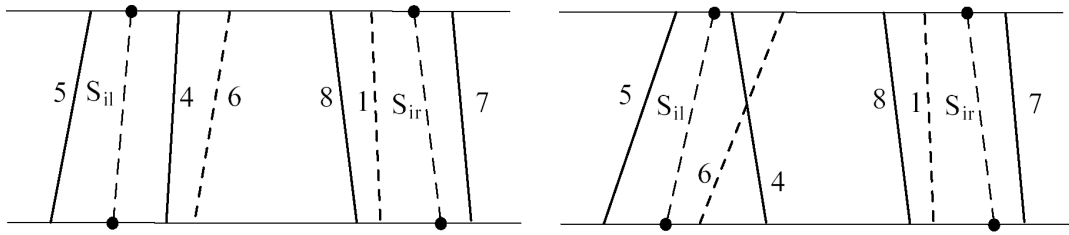


Fig. 25 - case \mathbf{a}_1 at both ends of the strip (left); case \mathbf{a}_1 at the top and \mathbf{a}_3 at the bottom (right)

Concluding, finding the feasibility set for polygonal silhouettes only requires finding the intersection of the feasibility sets computed at the y of the vertices.

8 CONCLUSIONS AND OPEN PROBLEMS

We have introduced and explored the problem of understanding the shape of 3D objects from silhouettes when the relative position of the viewpoints is not known, which happens in several practical cases.

In particular, the questions addressed are finding if a set of silhouettes is compatible with a real object, and constructing compatible objects. After discussing the problem in 2D, we have presented a necessary and sufficient condition for two orthographic silhouettes of 3D objects to be compatible. We have shown that pairwise compatibility is not sufficient for the compatibility of n silhouettes. Considering the object reconstructed has suggested a necessary and sufficient compatibility condition. This condition has been applied to the particular case of orthographic projections with viewing directions parallel to a plane. For this case, we have been able to work out sets of inequalities, involving the volume intersection parameters, which allow computing feasible solution sets. These inequalities allows to answer the two questions addressed: finding if a set of silhouettes is compatible with a real object, and in this case constructing compatible objects The number of the sets of inequalities, as well as the number of inequalities in each set, quickly

increases with the number of silhouettes. For practical applications, efficient computer algorithms for solving the sets of inequalities should be studied.

Several problems are open. Among them, the case of orthographic projection with unrestricted viewing directions, and the case of perspective projections. Other results could be obtained by dropping the restrictions of simply connected objects or mono-valued functions for defining the silhouettes. Practical algorithm could benefit by the shape of several real objects, which could allow finding correspondences between points of various silhouettes. This would restrict the degrees of freedom of VI, as in the cases of section 6.2 and 6.3. Finally, silhouette data and surface features could be integrated in practical algorithms.

Another question is worth considering. Except for special cases, as that of Fig. 9, we expect that infinite compatible objects exist, specified by a region in the space of the intersection parameters. Simple ways for describing the shape of the compatible objects seem desirable. For instance, is it possible to find hard points, that is points belonging to any compatible object? Another idea could be finding the maximum enclosed volume and the minimum finite bounding volume for all these objects.

Finally, at first glance it could seem that questions as those discussed could be raised for sets of silhouettes *without* the corresponding viewpoints. This would be the problem to face if we were given a set of images of an object taken with cameras with unknown parameters. In fact, these questions are neither practical nor fruitful. It is easy to see that any such set is compatible since infinite different compatible objects can be constructed for any set. For doing this it is sufficient to create, on the surface of a convex object, protrusions with appropriate shapes, each able to produce one silhouette of the set from a close viewpoint.

References

- [1] N. Ahuja and J. Veenstra: Generating octrees from object silhouettes in orthographic views, *IEEE Trans. on PAMI*, Vol.11, pp.137-149, 1989
- [2] K. Astrom and F. Kahl: Motion estimation in image sequences using the deformation of apparent contours, *IEEE Trans. on PAMI*, Vol. 21, No.2, pp.114-126, 1999
- [3] A. Bottino, L. Cavallero, A. Laurentini, "Interactive reconstruction of 3D objects from silhouettes," *Proc. WSCG '2001*, Vol.II, pp. 230-236, Plzen, February 5-9, 2001
- [4] E. Boyer and M. O. Berger, "3D Surface Reconstruction Using Occluding Contours," *Int'l. J. of Computer Vision*, vol.22, no.3, pp. 219-233, 1997
- [5] C. H. Chian and J. K. Aggarwal: Model reconstruction and shape recognition from occluding contours", *IEEE Trans. on PAMI*, Vol.11, pp.372-389, 1989
- [6] R. Cipolla and A. Blake, "Surface Shape from the Deformation of Apparent Contours," *Int'l. J. of Computer Vision*, vol.9, no.2, pp. 83-112, 1992
- [7] D. Dobkin, H. Edelsbrunner, C. K. Yap: Probing Convex Polytopes, *Proc. 18th ACM Symp. Theory of Computing*, 1986, pp. 424-432
- [8] A. Laurentini: The visual hull concept for silhouette-based image understanding," *IEEE Trans. on PAMI*, Vol. 16, No.2, pp. 150-162, 1994
- [9] A. Laurentini : How far 3-D shapes can be understood from 2-D silhouettes," *IEEE Trans. on PAMI*, Vol.17, No.2, pp.188-195, 1995
- [10] A. Laurentini: How many 2D silhouettes it takes to reconstruct 3D objects, *Computer vision and Image Understanding*, Vol.67, pp.81-87, 1997
- [11] S.Y.R. Li, Reconstructing polygons from projections, *Inform. Proc. Lett.* 28, pp. 235-240, 1988
- [12] M. Lindenbaum and A. Bruckstein, Reconstructing a convex polygon from binary perspective projections, *Pattern Recognition*, Vol.23, no.12, pp. 1343-1350, 1990

- [13] L.Jaulin and E.Walter: Guaranteed nonlinear set estimation via interval analysis, *Bounding Approaches to System Identification*, edited by M.Milanese et al, Plenum Press, New York, pp.363-381, 1996
- [14] M. Jones and J.P. Oakley: Registration of image sets using silhouette consistency, *IEE Proc.-Vis. Image Signal Process.*, Vol 147, No. 1, pp. 1-8, 2000
- [15] W. Matusik, et al.: Image based visual hulls, *Proc. ACM Siggraph 2000*,pp.369-374
- [16] P.R.S. Mendonca, K.K. Wong, and R. Cipolla,"Epipolar Geometry from Profiles under Circular Motion," *IEEE Trans. on PAMI*, Vol.23,no.6, pp.604-616, 2001
- [17] Noborio et al.:Construction of the octree approximating three-dimensional objects by using multiple views, *IEEE Trans. on PAMI*, Vol.10, pp.769-782,1988
- [18] M.Potemesil: Generating octree models of 3D objects from their silhouettes in a sequence of images, *Comput.Vision Graphics Image Process.*,Vol.40,pp.1-29,1987
- [19] S. Skiena: Interactive reconstruction via geometric probing, *IEEE Proc.*,Vol.80, No.9, pp1364-1383, 1992
- [20] S. Sullivan and J. Ponce:Automatic model construction and pose estimation from photographs using triangular splines, *IEEE Trans. on PAMI*,Vol.20,No.10,pp.1091-1097, 1998
- [21] R. Vaillant and O. Faugeras: Using extremal boundaries for 3D object modeling, *IEEE Trans. on PAMI*, Vol. 14, no.2, pp.157-173,1992
- [22] J. Y. Zheng: Acquiring 3D models from sequences of contours, *IEEE Trans. on PAMI*, Vol. 16, no.2, pp.163-178,1994